

Far-infrared optical properties of the carbide superconductor $\text{Y}_2\text{C}_2\text{I}_2$

T. Rööm,* B. Gorshunov,[†] and M. Dressel*1. Physikalisches Institut, Universität Stuttgart, Pfaffenwaldring 57, D-70550 Stuttgart, Germany*

K. Ahn, R. K. Kremer, and A. Simon

Max-Planck-Institut für Festkörperforschung, Heisenbergstraße 1, D-70569 Stuttgart, Germany

(Received 14 February 2002; published 8 July 2002)

The optical properties of the layered superconductor $\text{Y}_2\text{C}_2\text{I}_2$ ($T_c = 10$ K) have been studied at far-infrared frequencies down to 5 cm^{-1} and at temperatures from 5 to 15 K, in superconducting and normal states. A clear manifestation of the superconducting transition has been observed in the reflectance spectra and in the Kramers-Kronig derived spectra of conductivity and dielectric permittivity. The normal-state spectra indicate an unusually low scattering rate of the charge carriers.

DOI: 10.1103/PhysRevB.66.012510

PACS number(s): 74.70.Dd, 78.30.-j, 74.25.Gz

Compounds crystallizing with a layered structure display a wealth of exceptional and unusual properties. Recent examples include the high transition temperatures of the oxocuprate superconductors, magnesium diborate, or the large magnetoresistance in some layered compounds. Other superconductors with a layered structure and with quasi-two-dimensional properties were studied since the 1970s. Among them are the layered Ta and Nb dichalcogenides and their intercalated derivatives, or some organic superconductors, all of which display less spectacular transition temperatures. Since the seminal paper by Ginzburg and Kirznits,¹ it is generally accepted that two-dimensional layered materials provide optimum prerequisites for superconductivity with high T_c .^{2,3}

Some years ago we reported superconductivity in the layered carbide halides of the nonmagnetic rare-earth metals.⁴ The crystal structures of these compounds with general composition $R_2\text{C}_2\text{X}_2$ ($R = \text{Y, La}$; $X = \text{Br, I}$) contain slabs of close-packed R atom double layers with C_2 units occupying the octahedral voids of the metal atom double layers. These slabs are sandwiched by layers of halogen X atoms. Slabs of $X\text{-R-C}_2\text{-R-X}$ are connected via van der Waals interaction and stack along the crystallographic c axis.^{5,6} A superconducting transition temperature of 10 K has been found for $\text{Y}_2\text{C}_2\text{I}_2$. T_c could be maximized to 11.6 K by adjusting the electronic properties using an appropriate mixture of halide species in the compound $\text{Y}_2\text{C}_2\text{Br}_{0.5}\text{I}_{1.5}$ (Ref. 7). From measurements of the thermodynamic properties of $\text{Y}_2\text{C}_2\text{I}_2$ and $\text{Y}_2\text{C}_2\text{Br}_2$ ($T_c = 5$ K) a ratio $2\Delta/k_B T_c = 4.3$ has been established⁸ corresponding to a gap value, Δ , of the order of 2 and 1 meV respectively ($1\text{ meV} = 8.066\text{ cm}^{-1}$). So far there have been no reports on the direct measurements of the magnitude of the superconducting gap 2Δ in the carbide halides of the rare earth metals. In this paper we report on far-infrared (down to 5 cm^{-1}) measurements of $\text{Y}_2\text{C}_2\text{I}_2$ reflectance above and below T_c . We find evidence for a gap opening in the reflectance spectra. However, the reflectance spectra do not reveal the magnitude of the superconducting gap 2Δ .

Since single crystals of suitable quality, at least a few millimeters in size, are not available at present, the study was performed on polycrystalline pellets, 8 mm in diameter and 1 mm thick, pressed from a powder sample without additional

sintering. The typical size of crystallites in the pellets was 0.1 mm in the plane and about ten times less in the c direction. The powder sample was prepared by adding an excess of 3–4 % of amorphous carbon necessary to compensate for the loss of carbon due to its reaction with Ta crucible reaction container. X-ray diffraction from the powder (see the inset of Fig. 1) indicates the diffraction pattern of a monophasic sample. All reflections can be indexed on a basis of a monoclinic lattice of $\text{Y}_2\text{C}_2\text{I}_2$. Rietveld refinements of neutron-diffraction patterns (HRPT, SINQ) at 2 K indicated⁹ a composition of $\text{Y}_2\text{C}_x\text{I}_2$ with $x = 1.99 \pm 0.03$. The carbide halides of rare-earth metals are moisture sensitive. That is why the sample handling, including the mounting of the pellet on a far-infrared reflectance probe, has been done in a glove box filled with a dry argon atmosphere. The reflectance probe was transferred in a sealed container filled with dry argon gas to a cryostat precooled to 150 K. The cryostat was of a continuous-flow type, where the sample was cooled by a He heat exchange gas. During the reflectance measurements the sample temperature was always kept below 150 K. Below 40 cm^{-1} the reflectance was measured in a quasi-optical arrangement using backward-wave oscillators as sources of tunable coherent radiation.¹⁰ At higher frequencies, up to 10^4 cm^{-1} , a Fourier spectrometer Bruker IFS 113 v was used. The sample reflectance was compared to the reflectance of a reference mirror (aluminum film evaporated on a

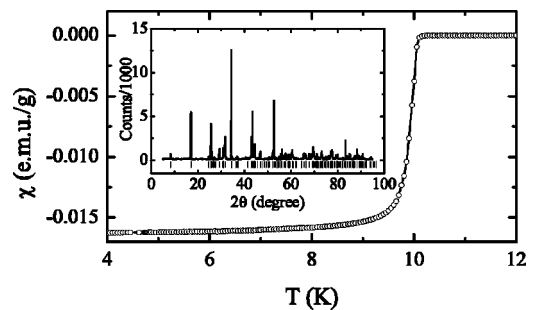


FIG. 1. Temperature dependence of the magnetic susceptibility measured in a 1 mT field while sweeping the temperature from 4 K up. The sample was cooled to 4 K in a zero magnetic field. The inset displays an x-ray-diffraction pattern of the investigated sample of $\text{Y}_2\text{C}_2\text{I}_2$.

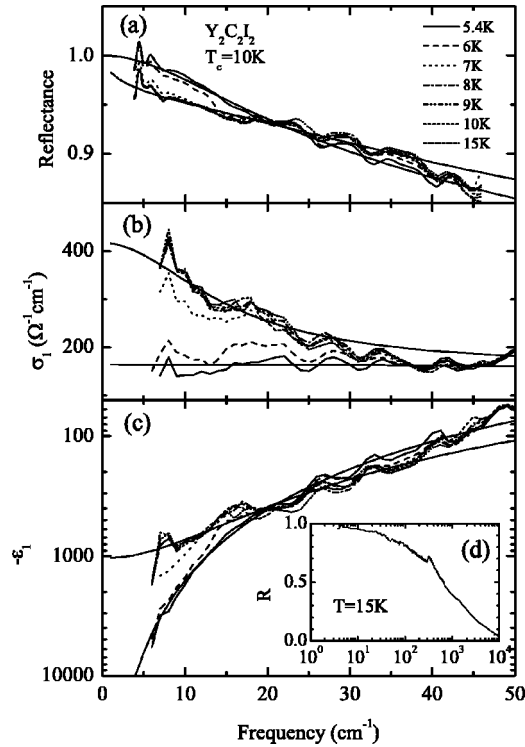


FIG. 2. Temperature and frequency dependences of the measured absolute reflectance and optical constants calculated using the Kramers-Kronig relation. (a) Low-frequency reflectance. (b) Real part σ_1 of the conductivity. (c) Real part ϵ_1 of the dielectric function multiplied by -1 . Inset (d) shows the reflectance measured at 15 K over a broad frequency range. A peak at $\approx 300 \text{ cm}^{-1}$ is a phonon (Refs. 16 and 17). Smooth solid curves are the model fits of 5.4- and 15-K spectra. The background conductivity at both temperatures is modeled with a Drude conductivity, $\omega_p = 1900 \text{ cm}^{-1}$ and $\Gamma = 400 \text{ cm}^{-1}$. In the normal state another Drude term has been added with $\omega_p = 480 \text{ cm}^{-1}$ and $\Gamma = 15 \text{ cm}^{-1}$, and in the superconducting state a delta peak with a plasma frequency $\omega_{ps} = 400 \text{ cm}^{-1}$.

glass substrate) by changing *in situ* the sample and the reference mirror on the back of a 4-mm-diameter aperture.

In Fig. 1 the magnetic gram susceptibility of a sample, prepared from the same batch as the one used for far-infrared measurements, is shown. The onset T_c is 10.1 K and the transition width (10–90 %) amounts to 0.7 K; the diamagnetic shielding is complete below 9 K, indicating a very good homogeneity of the sample. The absolute reflectance of $\text{Y}_2\text{C}_2\text{I}_2$ measured between 3 and 45 cm^{-1} is displayed in Fig. 2(a). Two peaks close to 5 cm^{-1} and oscillations above 25 cm^{-1} are due to standing waves in the cryostat. These features are temperature independent. By performing a Kramers-Kronig analysis of the reflectance spectra of $\text{Y}_2\text{C}_2\text{I}_2$, we calculated the real parts of the optical conductivity σ_1 and of the dielectric permittivity, ϵ_1 . In the analysis the high-frequency reflectance spectrum [Fig. 2(d)] was measured up to 10^4 cm^{-1} , and beyond this frequency a power-law extrapolation $a\omega^{-2} + b\omega^{-4}$ was used; the low-frequency extrapolation below 3 cm^{-1} was calculated using a Hagen-Rubens relation. Surface roughness, inherently present in pressed polycrystalline samples, reduces the reflectance in

the infrared. We found that this reduction leads to a frequency-independent lowering of the conductivity in the far-infrared frequency range of our main interest, below 50 cm^{-1} ; thus it does not affect the qualitative features seen in the spectra of $\sigma_1(\omega)$ and $\epsilon_1(\omega)$.

The low-frequency part of the conductivity and permittivity spectra obtained by the Kramers-Kronig analysis are shown in Figs. 2(b) and 2(c). In the normal state an increase of the conductivity toward low frequencies is seen, characteristic of a Drude-like response of free charge carriers. A corresponding drop is observed in the $\epsilon_1(\omega)$ spectrum. This Drude-like dispersion seen in the conductivity and permittivity spectra in the normal state indicates an unexpectedly low scattering rate of the charge carriers, $\Gamma \approx 15 \text{ cm}^{-1}$. Taking the Fermi velocity $v_F = 10^5 - 10^6 \text{ m/s}$ we estimate the mean free path $l = v_F/\Gamma$ to be $l = 0.2 - 2 \text{ }\mu\text{m}$. This is larger than the distance between two Y layers across the van der Waals gap [less than 1 nm (Ref. 11)], but still smaller than the dimensions of the crystallites in the pellet. The direct current conductivity of a pressed pellet at 15 K $\sigma_1(0) = 1000 \text{ }\Omega^{-1} \text{ cm}^{-1}$ (Ref. 12) is slightly larger than the low frequency optical conductivity, $\sigma_1(10 \text{ cm}^{-1}) = 400 \text{ }\Omega^{-1} \text{ cm}^{-1}$. We attribute this difference to the light scattering effects.

In the superconducting state a strong decrease of $\epsilon_1(\omega)$ at the lowest frequencies develops corresponding to an inductive response of the superconducting condensate under the zero-frequency delta function in the conductivity spectrum. This is accompanied by a pronounced lowering of the conductivity. The conductivity, however, does not fall to zero at the lowest frequencies, as one would expect at $T \ll T_c$ for a superconductor in which the gap opens over the entire Fermi surface, leading to a zero conductivity below the gap frequency. Instead, a flat background conductivity of about $150 \text{ }\Omega^{-1} \text{ cm}^{-1}$ remains even at the lowest temperature of 5.4 K. The origin of such a residual conductivity can be extrinsic or intrinsic. There are arguments against an extrinsic origin of this contribution in the superconducting state. *First*, we exclude the presence of other phases. Although a few percent extra carbon were added in the sample, the x-ray and neutron diffraction do not show the presence of other phases. Even if the extra carbon could still be present in the sample in an amorphous form, it would not give rise to a relatively large metal-like conductivity because of the low value of the conductivity.¹³ *Second*, disorder or localization effects, which could give rise to a residual conductivity below T_c , lead to an increase of the conductivity with frequency according to a ω^s power law and to a positive ϵ_1 with a divergence as $\omega \rightarrow 0$ (Ref. 14), a behavior not observed in our spectra. Also, in the normal state there is an opposite, as compared to ω^s , behavior of the conductivity [Fig. 2(b)].

Assuming that the features we observe in the low-frequency spectra of $\text{Y}_2\text{C}_2\text{I}_2$ are intrinsic, we can draw an analogy to another recently discovered layered superconductor MgB_2 . We modeled the normal-state optical conductivity of $\text{Y}_2\text{C}_2\text{I}_2$ with a Drude-Lorentz conductivity, a sum of two conductivity peaks, $\sigma_i(\omega) = \sigma_{dc,i} \Gamma_i^2 / (\omega^2 + \Gamma_i^2)$ (see Fig. 2). One conductivity peak is narrow, $\Gamma_1 \approx 15 \text{ cm}^{-1}$, and the

other is broad, $\Gamma_2 \approx 400 \text{ cm}^{-1}$. In MgB_2 two very similar Drude-like contributions are detected (see, e.g., Ref. 15), a narrow one with a width determined by a small scattering rate of about 30 meV (240 cm^{-1}), and a very broad one with scattering rate of 1.39 eV (11200 cm^{-1}). These two components in MgB_2 are regarded as originating from two different electronic bands, each participating in producing two superconductivity channels with different energy gaps (or with a distribution of gap values). We can thus speculate on a possibility of a similar two-band conductivity and superconductivity in $\text{Y}_2\text{C}_2\text{I}_2$. Recent band-structure calculations¹⁶ indicate the possibility of such a multiband conductivity mechanism in $\text{Y}_2\text{C}_2\text{I}_2$. Certainly, for a more detailed analysis, further experiments on single crystalline samples are needed.

As indicated above, the delta peak of superconducting carriers at zero frequency in $\sigma_1(\omega)$ adds a large negative contribution to $\epsilon_1(\omega)$, $\epsilon_1^{\text{sc}}(\omega) = -(\omega_{pl}^{\text{sc}}/\omega)^2$. In the low-frequency limit $\omega \rightarrow 0$, the plasma frequency of superconducting carriers can be estimated as $\omega_{pl}^{\text{sc}} = \omega \sqrt{|\epsilon_1^{\text{sc}}(\omega)|}$. At 5.4 K we obtain $\omega_{pl}^{\text{sc}} = 400 \text{ cm}^{-1}$. According to our model fit the spectral weight of a narrow Drude conductivity peak in the normal state is approximately of the same size, $\omega_{pl} = 480 \text{ cm}^{-1}$. Therefore, it is reasonable to assume that the charge carriers in the narrow Drude peak condense into a delta peak conserving the spectral weight when the sample becomes superconducting. Using these two values we obtain the London penetration depth $\lambda_L = (2\pi\omega_{pl}^{\text{sc}})^{-1}$ in a range from 3.3 to 4 μm . From the transverse-field muon spin relaxation study the in-plane London penetration depth $\lambda_L^{\parallel} = 0.26 \mu\text{m}$ was obtained.¹⁸ An estimate of the out-of-plane penetration depth λ_L^{\perp} , using an anisotropy ratio 5.2, based on the investigation of the upper critical field,¹⁸ can be done. For the out-of-plane penetration depth we obtain $\lambda_L^{\perp} = 5.2\lambda_L^{\parallel} = 1.3 \mu\text{m}$. It is not surprising that the penetration depth determined from the optical properties measured on a polycrystalline sample is larger than the in-plane value. In the polycrystalline sample both directions, in plane and out of plane, are probed and the average is observed. In HTCS materials it turned out that the reflectance and the Kramers-Kronig-derived optical conductivity of polycrystalline samples¹⁹ were almost like pure out-of-plane properties.²⁰ In the extreme limit we can assume the measured optical properties of the polycrystalline $\text{Y}_2\text{C}_2\text{I}_2$ are properties perpendicular to the highly conducting planes as well. Then the anisotropy ratio is 15–20 according to the muon spin relaxation in-plane value 0.26 μm , and the optical out-of-plane value is 3.3–4 μm . A similar situation was encountered in HTCS materials, where from the critical field measurements an anisotropy ratio of 6 was deduced,²¹ while according to optical measurements^{20,22} it was approximately 40. The large out-of-plane penetration depth could be explained by the large effective mass of the charge carriers in the direction perpendicular to the planes where the conduction band has a small dispersion.

To obtain a clearer picture of the evolution of the optical properties of $\text{Y}_2\text{C}_2\text{I}_2$ with temperature, in Fig. 3 we plot the ratio of the reflectance and the conductivity measured at tem-

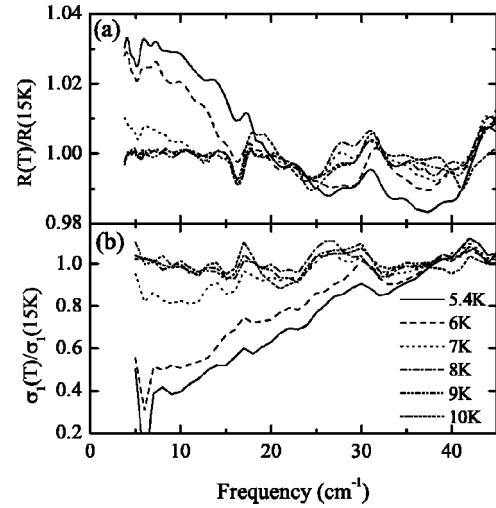


FIG. 3. The frequency and temperature dependences of the reflectance ratio (a) and of the conductivity ratio (b).

perature T to those measured at 15 K (in the normal state). We see that the reflectance does not change between 15 and 8 K. Below 8 K there is a gradual increase in the ratio toward lower frequencies starting at 20 cm^{-1} . Above this frequency the reflectance is lower in the superconducting state than in the normal state. The reflectance ratio crosses unity at 20 cm^{-1} at 5.4 K. The crossing point shifts to lower frequencies as the temperature rises. At 8 and 9 K, where the sample is still superconducting, the unity crossing of the reflectance ratio may lie below our low-frequency limit of 5 cm^{-1} . Unity crossing in R_{sc}/R_n occurs at the same frequency where the normal and superconducting states ϵ_1 cross [Fig. 2(c)]. Therefore, the observed unity crossing in R_{sc}/R_n is an interplay of the narrow Drude peak in the normal state and of the superconducting delta peak contribution to the dielectric permittivity.

Although a very pronounced decrease of the conductivity is seen in the superconducting state [see Fig. 2(b)], indicative of an energy gap opening, an extraction of the value of 2Δ cannot be done because of a residual contribution to the conductivity. We can try to obtain information about the gap value from the reflectivity ratio R_{sc}/R_n . Within the BCS formalism, the spectrum of R_{sc}/R_n peaks at 2Δ for the dirty limit ($\tau^{-1} \gg 2\Delta$) superconductor, while in the clean limit the peak broadens considerably, making its assignment to a gap feature difficult.²³ For example, the gap obtained from the reflectance ratio was recently reported in another carbide superconductor $\text{Lu}(\text{Ni}_{1-x}\text{Co}_x)_2\text{B}_2\text{C}$, which, due to the substitution of cobalt for nickel, is put in the dirty limit.²⁴ The reflectance ratios measured for $\text{Y}_2\text{C}_2\text{I}_2$ are presented in Fig. 3(a). As the figure shows, there is no maximum observed at any temperature, although a flattening is clearly detected in the spectra around 7 cm^{-1} in the superconducting state. This is consistent with the behavior of the conductivity ratio [Fig. 3(b)], where no minimum is observed down to the lowest frequency. The optical gap in $\text{Y}_2\text{C}_2\text{I}_2$ is expected to be $2\Delta = 30 \text{ cm}^{-1}$ based on the estimate of $2\Delta/k_B T_c = 4.3$ from

the thermodynamic properties.⁸ We suggest that the gap feature in R_{sc}/R_n is not observed because $Y_2C_2I_2$ is in the clean limit.

In conclusion, we have studied the optical low-frequency electrodynamic response of a polycrystalline superconducting sample of $Y_2C_2I_2$. We have detected the superconducting transition as an increase of the reflection coefficient and as a strong decrease of the dielectric permittivity and conductivity in the superconducting state. In the superconducting state and at the lowest frequencies a finite frequency independent conductivity is observed whose origin is presumably related to the two-band conductivity process. From the dielectric permittivity spectrum we have determined the London pen-

etration depth $\lambda_L = 4 \mu\text{m}$, and the plasma frequency of the superconducting condensate $\omega_{pl}^{sc} = 400 \text{ cm}^{-1}$. Our findings are indicative of a clean limit superconductivity in $Y_2C_2I_2$. In the normal state the spectra of conductivity and permittivity show features of a Drude-like response with an unexpectedly low scattering rate of about 15 cm^{-1} . Further measurements at the single crystalline samples are needed to clarify an unusual low-frequency electrodynamic of $Y_2C_2I_2$.

We thank J. Kortus and O. Dolgov for helpful discussions, and P. Haas for technical support during the infrared experiments. T.R. gratefully acknowledges the financial support from the Max Planck Society.

*Permanent address: National Institute of Chemical Physics and Biophysics, Akadeemia tee 23, 12618 Tallinn, Estonia. Email address: roomtom@kbfi.ee

[†]Permanent address: General Physics Institute, Russian Academy of Sciences, Moscow, Russia.

¹V.L. Ginzburg and D.A. Kirznits, Zh. Éksp. Teor. Fiz. **46**, 397 (1964) [Sov. Phys. JETP **19**, 269 (1964)].

²*High-Temperature Superconductivity*, edited by V. L. Ginzburg and D. A. Kirznits (Plenum, New York, 1982).

³T. H. Geballe, in *Physics of High-Temperature Superconductors*, edited by S. Maekawa and M. Sato, Springer Series in Solid-State Sciences Vol. 106 (Springer-Verlag, Berlin, 1992), p. 339; T. H. Geballe, Science **259**, 1550 (1993).

⁴A. Simon, H.J. Mattausch, R. Eger, and R.K. Kremer, Angew. Chem. Int. Ed. Engl. **30**, 1188 (1991).

⁵U. Schwanitz-Schüller and A. Simon, Z. Naturforsch. B **40**, 710 (1985).

⁶H.J. Mattausch, R.K. Kremer, R. Eger, and A. Simon, Z. Anorg. Allg. Chem. **609**, 7 (1992).

⁷A. Simon *et al.*, Z. Anorg. Allg. Chem. **622**, 123 (1996).

⁸W. Schnelle, R.W. Henn, Th. Gulden, R.K. Kremer, and A. Simon, J. Appl. Phys. **83**, 7321 (1998).

⁹K. Ahn *et al.* (unpublished).

¹⁰G. V. Kozlov and A. A. Volkov, in *Millimeter and Submillimeter Wave Spectroscopy of Solids*, edited by G. Grüner (Springer-Verlag, Berlin, 1998), p. 51.

¹¹H.J. Mattausch, H. Borrmann, and A. Simon, Z. Kristallogr. **209**, 281 (1994).

¹²R.W. Henn, W. Schnelle, R.K. Kremer, and A. Simon, Phys. Rev. Lett. **77**, 374 (1996).

¹³K. Shimakawa and K. Miyake, Phys. Rev. B **39**, 7578 (1989).

¹⁴N. F. Mott, *Metal-Insulator Transitions* (Taylor and Francis, New York, 1990); N.F. Mott and M. Kaveh, Adv. Phys. **34**, 329 (1985); N. F. Mott and E. Davis, *Electronic Processes in Non-Crystalline Materials* (Clarendon, Oxford, 1979); P.A. Lee and T.V. Ramakrishnan, Rev. Mod. Phys. **57**, 287 (1985); Kwanghee Lee, Reghu Menon, C.O. Yoon, and A.J. Heeger, Phys. Rev. B **52**, 4779 (1995).

¹⁵A.B. Kuz'menko *et al.*, cond-mat/0107092 (unpublished).

¹⁶P. Puschnig, C. Ambrosch-Draxl, R.W. Henn, and A. Simon, Phys. Rev. B **64**, 024519 (2001).

¹⁷R.W. Henn, T. Strach, R.K. Kremer, and A. Simon, Phys. Rev. B **58**, 14 364 (1998).

¹⁸R.W. Henn *et al.*, Phys. Rev. B **62**, 14 469 (2000).

¹⁹D.A. Bonn *et al.*, Phys. Rev. Lett. **58**, 2249 (1987).

²⁰C.C. Homes *et al.*, Phys. Rev. Lett. **71**, 1645 (1993).

²¹Ruixing Liang, P. Dosanjh, D.A. Bonn, W.N. Hardy, and A.J. Berlinsky, Phys. Rev. B **50**, 4212 (1994).

²²D.N. Basov *et al.*, Phys. Rev. Lett. **74**, 598 (1995).

²³See, for example, T. Timusk *et al.*, Phys. Rev. B **38**, 6683 (1988).

²⁴M. Windt *et al.*, Phys. Rev. B **65**, 064506 (2002).